Fermi National Accelerator Laboratory

TM-1558

Response of the D0 Muon Chamber to Changes in Voltage, Incident Angle, Gas Composition, and Oxygen Contamination

N. Oshima and S. Igarashi
Fermi National Accelerator Laboratory
P.O. Box 500, Batavia, Illinois

February 24, 1989

Operated by Universities Research Association, Inc., under contract with the United States Department of Energy

TM-1558

RESPONSE OF THE D0 MUON CHAMBER TO CHANGES IN VOLTAGE, INCIDENT ANGLE, GAS COMPOSITION, AND OXYGEN CONTAMINATION

N. Oshima S. Igarashi

February 24, 1989

Fermi National Accelerator Laboratory
P.O. Box 500, Batavia, Illinois 60510

Abstract

The measured space point resolution of a D0 Muon Chamber is ± 0.31 mm perpendicular to the anode wire and ± 2.7 mm parallel to the wire. A voltage change of 1 kV, which changes the gas gain by a factor of 50, only causes a change of drift velocity of 12 %. Tracks inclined of 45° have a resolution worse than those of 0° by a factor 3 ± 2. A change in gas composition from CO_2(10%) to CO_2(11%) decreases the gas gain by 17 ± 5 %, and decreases drift velocity by 0.2 ± 0.2 %. The effect of an oxygen contamination of 3200 ppm is to change of the mean pulse height by 45 % over the 5 cm width of the cell.

1. Introduction

A full length (5.5 m) D0 muon chamber with only nine cells was constructed in order to continue measurements of full length cells. The narrow chamber allowed easy rotation for measuring wide angle tracks and allowed quick gas flushing for measuring gas composition sensitivity. The cell structure and front end electronics are identical to standard muon chambers [Ref. 1 and 2].

The muon chamber, which is a proportional drift tube (PDT), is a 10 cm wide aluminum drift tube with shaped cathode pads 2 cm from the anode wire [Fig. 1]. The pulse arrival time difference at the two ends of the anode wire provides a rough longitudinal coordinate. The ratio of the charge induced on the cathode pads is then used for a precise longitudinal position. Drift time is measured for the coordinate perpendicular to the wire. The nominal gas mixture is 90 % Argon , 10 % CO_2 [Ref. 3] and the nominal operating voltages are + 4.54 kV on the anode wire, + 2.60 kV on the cathode pads, and ground potential on the aluminum tubes.

2. Set-up and Data Acquisition system

The test module was mounted on a rotator which was fixed on a steel table [Fig. 2]. This table has a fiducial mark to line up the test module and an external proportional wire chamber stand for external tracking. This stand has two FNAL beam line PWC's [Ref. 4] separated by 67 cm. The PWC's cover 128 mm (1 mm spacing) which spans the 10 cm drift cell.

The chamber was flushed continuously at $\approx$ 200 cc/min, and the gas was monitored with two analyzers during this study. An infrared gas analyzer (ANARAD, Inc.) monitored CO_2 (0-25%) and an oxygen analyzer (CUSTOM SENSORS AND TECHNOLOGY, INC.) monitored O_2 contamination. The gas monitoring system can get a sample from the input, the output, and from the standard calibration gases [Fig. 3].

The data acquisition system was a CAMAC based system (a TRANSIAC 6002 Microprocessor-CAMAC interface and a LeCroy 3512 Buffered ADC)

with an IBM/PC-XT. A homemade CAMAC interface (Cosmic Rat Controller) controlled the data flow from the front end electronics into the ADC. After all analog signals were loaded, digitized and stored in the ADC's memory, a LAM was generated to begin transfer of the digital signals from the ADC to the IBM/PC.

The trigger consisted of a coincidence between the two scintillators shown in Fig. 2. A single track in the PWC system was required in the data acquisition program.

3. Drift Time and Pulse Propagation Time (Δ T) Measurment

Operating voltages for the cells were determined by three factors, drift time, gas gain, and uniformity of collected ionization. A higher wire to pad voltage will increase gas gain, while a higher pad to ground voltage will increase drift velocity. The nominal operating voltages were chosen to give fairly uniform collected ionization, a nearly uniform drift velocity, and gas gain well separated from the streamer mode. The operating voltage plateaus of singles rates for cosmic ray triggers are shown in Figure 4. For these different sets of operating voltages, the corresponding drift velocities were measured [Fig. 5-a]. The gas Ar(90 %) + CO_2(10 %) is not saturated but is relatively insensitive, $(\Delta v_d/v_d)/V_{pad} \approx 12$ %/kV. The pad pulse heights were also measured using ^{241}Am and ^{55}Fe sources as a function of the wire high voltage [Fig. 5-b]. Clearly, the gas gain depends largely on the wire to pad voltage difference. The gain is exponentially related to this difference with coefficient 4 $(kV)^{-1}$, i.e. a change of supply by 250 volts causes a gain change of **e**.

The drift velocity was determined by reconstructing tracks with the two PWC's and comparing the projected track position in the PDT cell to the measured drift time as shown in Figure 6. In this figure one pixel size corresponds to 800 μm in space. The PWC resolution was $\pm$ 0.3 mm or almost one pixel. Obviously, a linear time to distance relation is a reasonable first order fit, and the slope of that fit was plotted in Figure 5-a.

The measured spatial resolution in the drift direction was found to be $\pm$ 0.31 mm [Fig. 7] after unfolding the result of using the three cells shown in Figure 2. Since non-linearities of order $\pm$ 0.4 mm are seen in Figure 6, a non-linear fit to the space-time relation was performed for the residual distribution of Figure 7. If a linear space-time relationship is assumed, the resolution appears to be $\pm$ 0.38 mm. This resolution of non-linear fitting is close to the diffusion limit of $\approx \pm$ 0.2 mm.

Figure 8 shows the resolution in the drift direction as a function of the angle of inclination. In this case the PWC's were used to predict the position in the middle layer cell shown in Figure 2. The unfolded result of $\pm$ 0.34 mm at 0° angle is consistent with the previous result. The spatial resolution degrades by a factor 3 $\pm$ 2 at 45°. It is consistent with no effects. The straight line in Fig. 8 is

σ(mm) = 0.278 + 0.018 θ(degrees).

The origin of this effect is not understood at present.

We also looked at the efficiency of the PDT as a function of position. We required hits in both top and middle layer cells and then looked for a hit in the bottom layer cell. The efficiency as a function of drift distance is shown in Figure 9. Clearly the effects of the aluminum wall (0.25 cm) are seen at the distance 5 cm from the wire. We found an efficiency greater than 96 $\pm$ 1 % for the PDT except the region 0.2 cm from the wall. Note those tracks were at normal incidence, which is presumably the worst case.

The time difference along the anode wire was used to get a rough longitudinal coordinate. The resolution was measured by using scintillators moved to different positions along the wire. Since the signals are attenuated by the wire resistance and the rise time degrades along the wire, there is a change in the resolution from one end of the wire to the other. In addition, in order to locate the chamber electronics all at one end of a chamber, anode wire pairs are jumpered together at the far end, so the effective length of a wire is twice the module length. The spatial resolution using the time difference

measurements ranges from ± 9 cm at the far end to ± 23 cm at the electronics end. This resolution is sufficient to resolve which pad repeat pattern (see Fig. 1-b) was hit.

4. Charge Ratio Measurment

Once the rough longitudinal coordinate has been measured, a precise longitudinal position is found from the charge ratio induced on the shaped cathode pads shown in Figure 1-b. A given charge ratio corresponds to two possible positions for every 60.9 cm along the pad, because the repetition length of the pads is 60.9 cm. To measure the resolution of the cathode pads the PWC's were translated to record the track position along the wire. Figure 10 shows the relationship between charge ratio and position. A linear relationship is also shown, which indicates that it is a reasonable first apporoximation. The spread of the points is an indication of the resolution. In Figure 11 we show a fit to the residuals indicating a resolution of ± 2.7 mm. This resolution corresponds to a measurement of the two pad charges with an accuracy of ± 1.3 %.

5. Effects of the CO_2 ratio

Three different gas compositions were run to measure the gas gain and the drift time sensitivity. Figure 12 shows the relatively large gain sensitivity (40 % gain change between 8.4 % and 11.0 % CO_2). To set the scale, a 1 % CO_2 change makes a 17 ± 5 % gain change which is equivalent to a voltage fluctuation of about 40 volts. Figure 13 shows the drift velocity for the three compositions. The slope is $\Delta v_d = 0.01$ cm/μsec per 1 % CO_2 change. The data is also consistent with no change within errors.

6. Oxygen Contamination Study

Oxygen contamination tests were performed at 150, 560, 1300, 2200 and 3200 ppm of oxygen. In Figure 14 we show the pulse height relative to the data at 150 ppm (i.e. no O_2) as a function of drift distance. Clearly there is a drop of $\approx$ 35 % in effective gas gain near the wire at 3200 ppm O_2. As

we see from Figure 5-b, that drop could be mimicked by a supply voltage drop of about 125 volts. However, there is more than a factor two loss at 5 cm drift distance, indicating attachment of the ionization. In figure 15 we show the gain near the wire as a function of O_2 contamination and the gain at maximum drift distance. Clear attachment effects are seen, which can be used to distinguish voltage variations from change in gas composition.

Acknowledgements

We are indebted to J. Sasek, G. Sellberg and R. Cantal for their technical support and to A. Tseng and P.Lee for their electrostatics calculations of the PDT which are used in Figure 1-a. We also would like to take the opportunity to acknowledge the encouragement by D. Green, H. Haggerty and R. Yamada during this work.

FigureCaptions

1. a) Cross section of the proportional drift tube (PDT) showing equipotential lines and b) a shaped cathode pad.

2. Test module set-up with the PWC stand.

3. Gas system for the test module.

4. Cosmic ray singles rate measurement as a function of high voltage.

5. a) Drift velocity and b) pad pulse height measurements as a function of high voltage.

6. Drift time as a function of the distance from the wire. The straight line is a first order fitting line.

7. Spatial resolution as determined from three drift time measurements.

   Using the determined drift velocity by the external PWC's and drift times, we measured three coordinates P_{top}, P_{mid} and P_{bot} on drift direction at each layer. These three coordinates have a common reference origin and should be equal.

   The residual R was defined as:

   $R = P_{mid} - (P_{top} + P_{bot})/2$

   $\delta R = (\delta P_{mid})^2 + ((\delta P_{top})^2 + (\delta P_{bot})^2)/4$

   If we assumed, $\delta P = \delta P_{top} = \delta P_{mid} = \delta P_{bot}$:

   $(\delta R)^2 = (\delta P)^2(1+2/4)$

   $(\delta P)^2 = (0.378\text{mm})^2(2/3)$

   $\underline{\delta P = 0.31 \text{ mm}}$

8. Spatial resolution as a function of track angles.

9. Efficiency as a function of drift distance.

10. Charge ratio as a function of position along the wire. Also shown is a linear relationship between position and charge ratio.

11. Spatial resolution of the charge ratio measurement.

12. Pad pulse height distribution with various Argon CO_2 mixture; CO_2 of 8.4, 10 and 11 %.

13. Drift velocity with 8.4 %, 10 % and 11 % CO_2 (Balance Argon)

14. Relative mean pad pulse height as function of distance from the wire for different oxygen contamination fractions 150, 560, 1300, 2200 and 3200 ppm.

15. Variation of pulse height near the wire and far from the wire as a function of oxygen contamination.

References

1. Design report, The D0 Experiment at the Fermilab Antiproton-Proton Collider. (1984).

2. Green, D. et al. "Accurate 2 Dimensional Drift Tube Readout Using Time Division and Vernier Pads." NIM A256, 305 (1987).

3. Green, D. et al. "Fast Non-explosive Gases." Fermilab TM-1523 (1988).

4. Fenker, H. "A Standard Beam PWC for Fermilab." TM-1179 (1983).

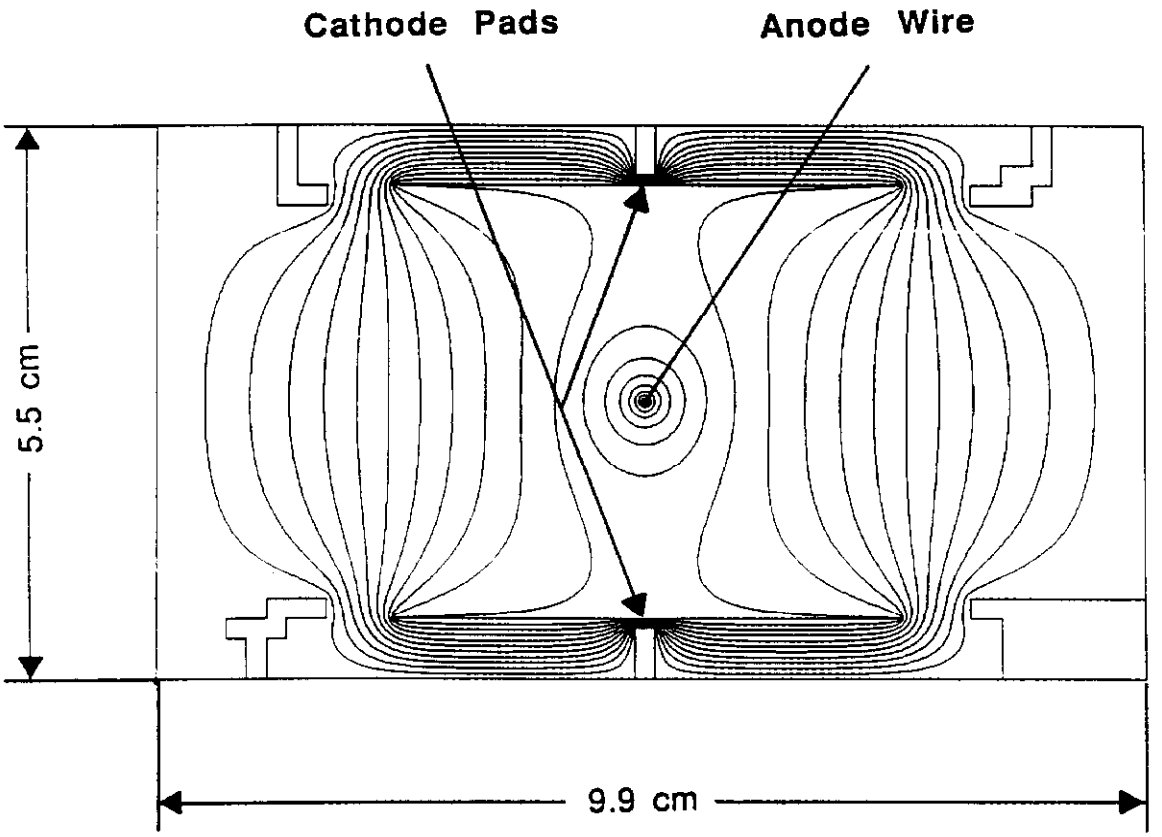

Fig. 1-a

[Shaped Cathode Pad]

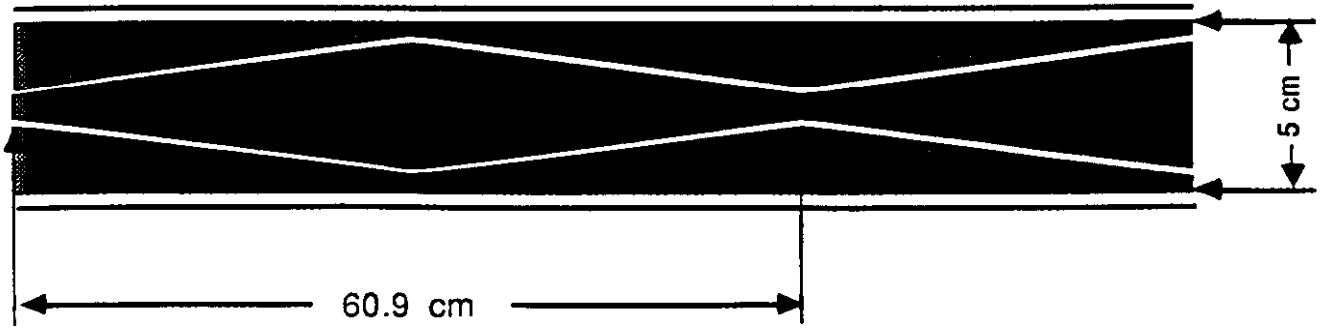

Fig. 1-b

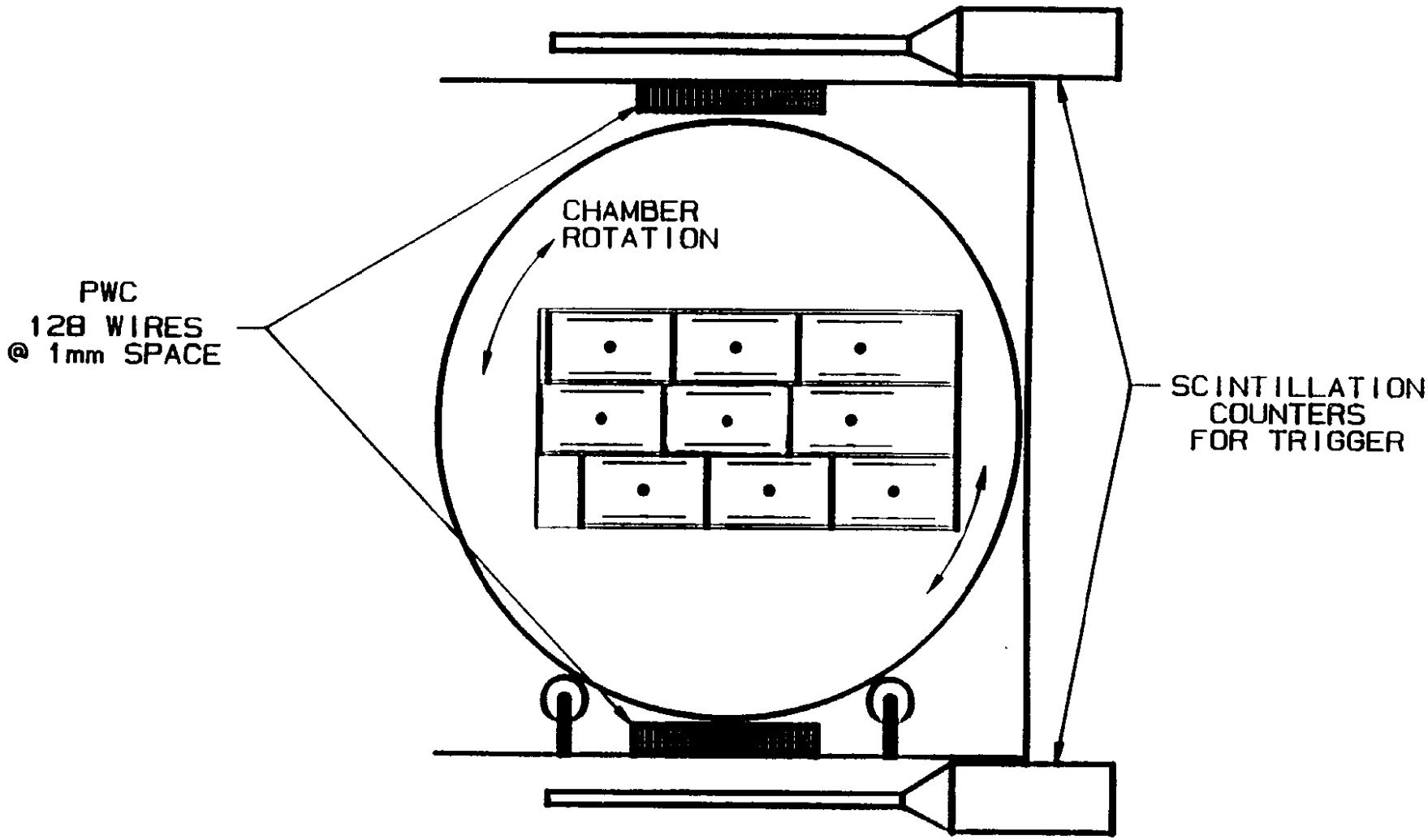
CHAMBER
ROTATION
PWC
128 WIRES
@ 1mm SPACE
SCINTILLATION
COUNTERS
FOR TRIGGER

Fig. 2

Oxygen Contamination Test Set-up

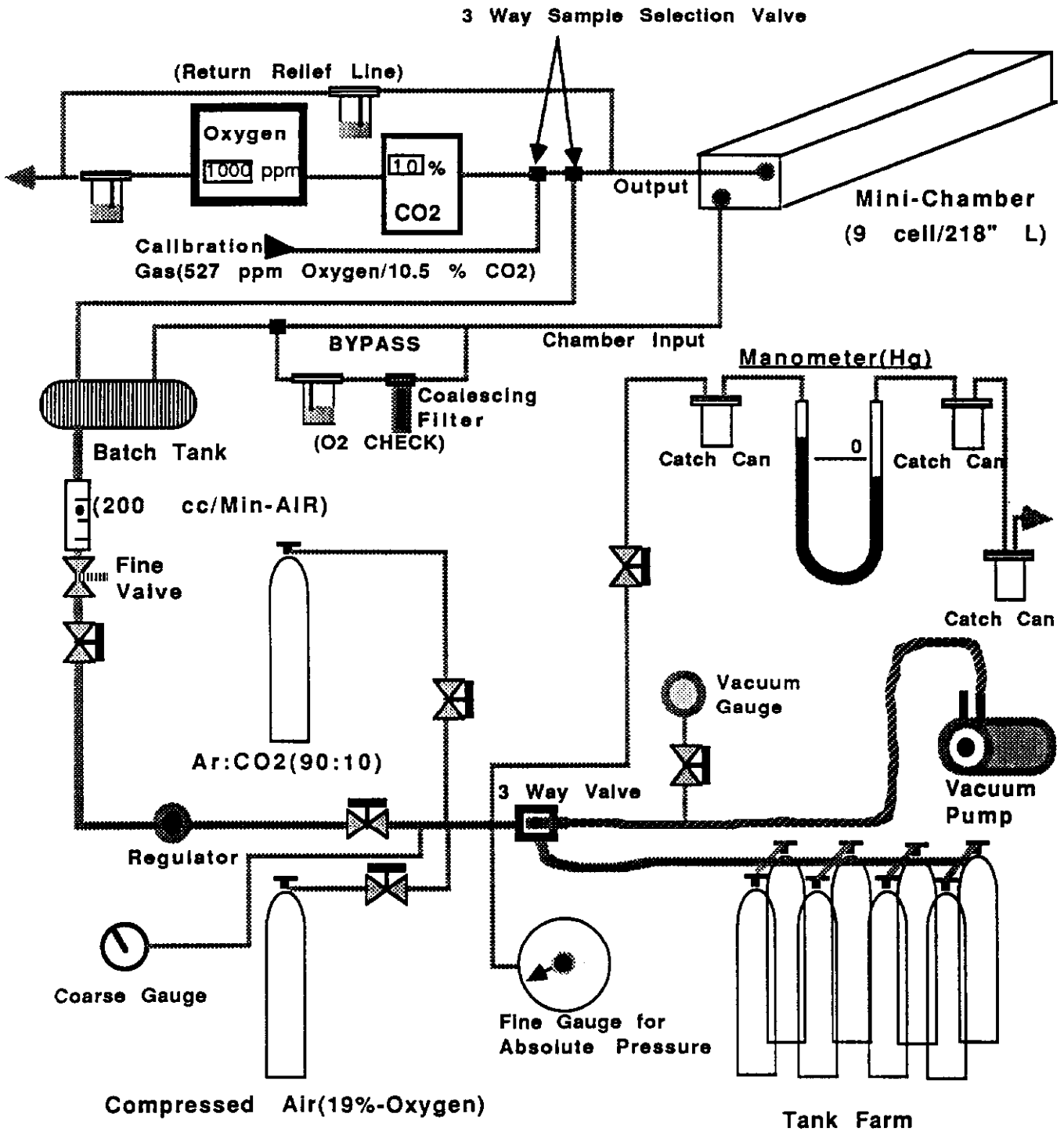

Fig. 3

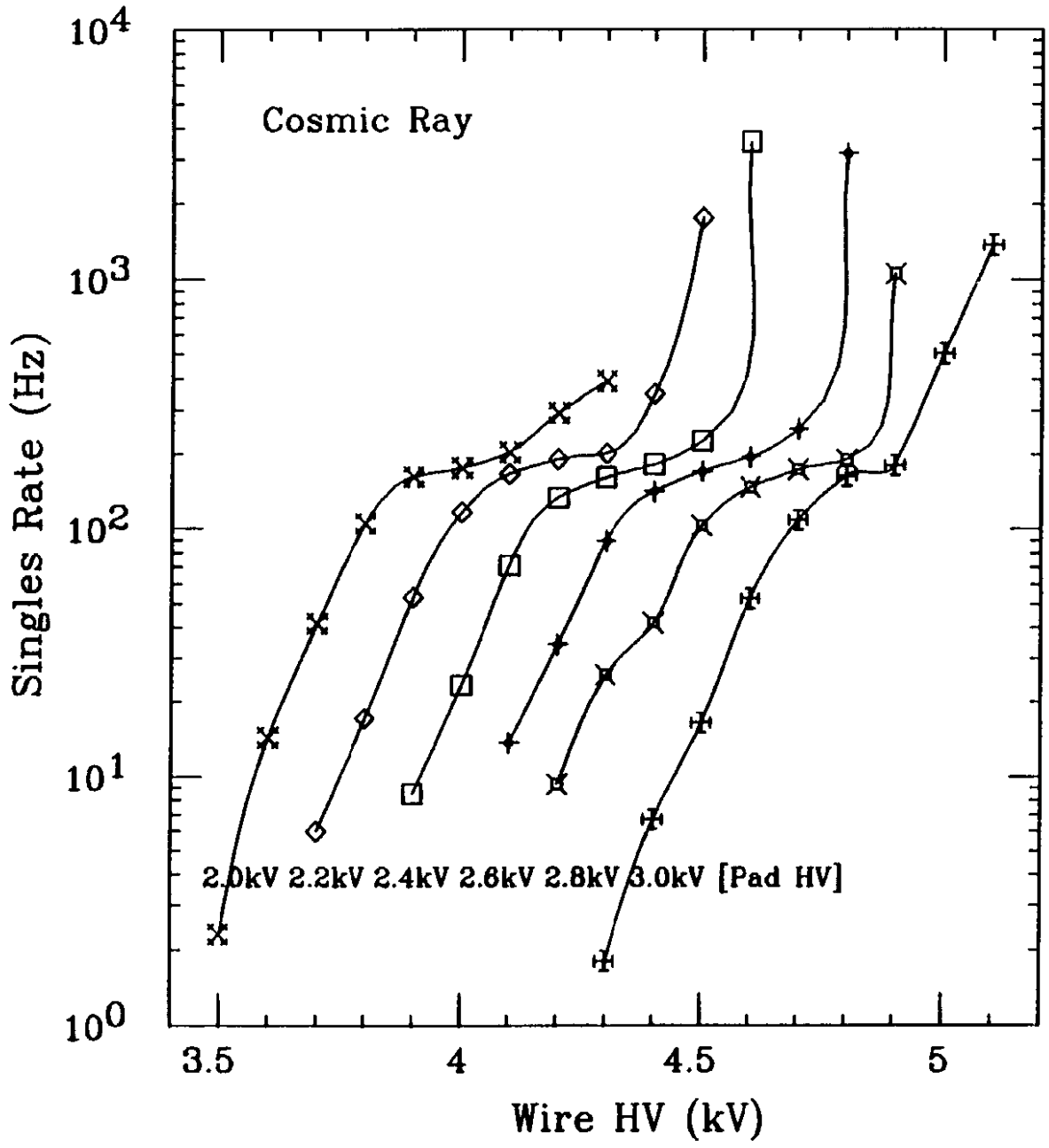
Cosmic Ray
Singles Rate (Hz)
10^4
10^3
10^2
10^1
10^0
2.0kV 2.2kV 2.4kV 2.6kV 2.8kV 3.0kV [Pad HV]
3.5
4
4.5
5
Wire HV (kV)

Fig. 4

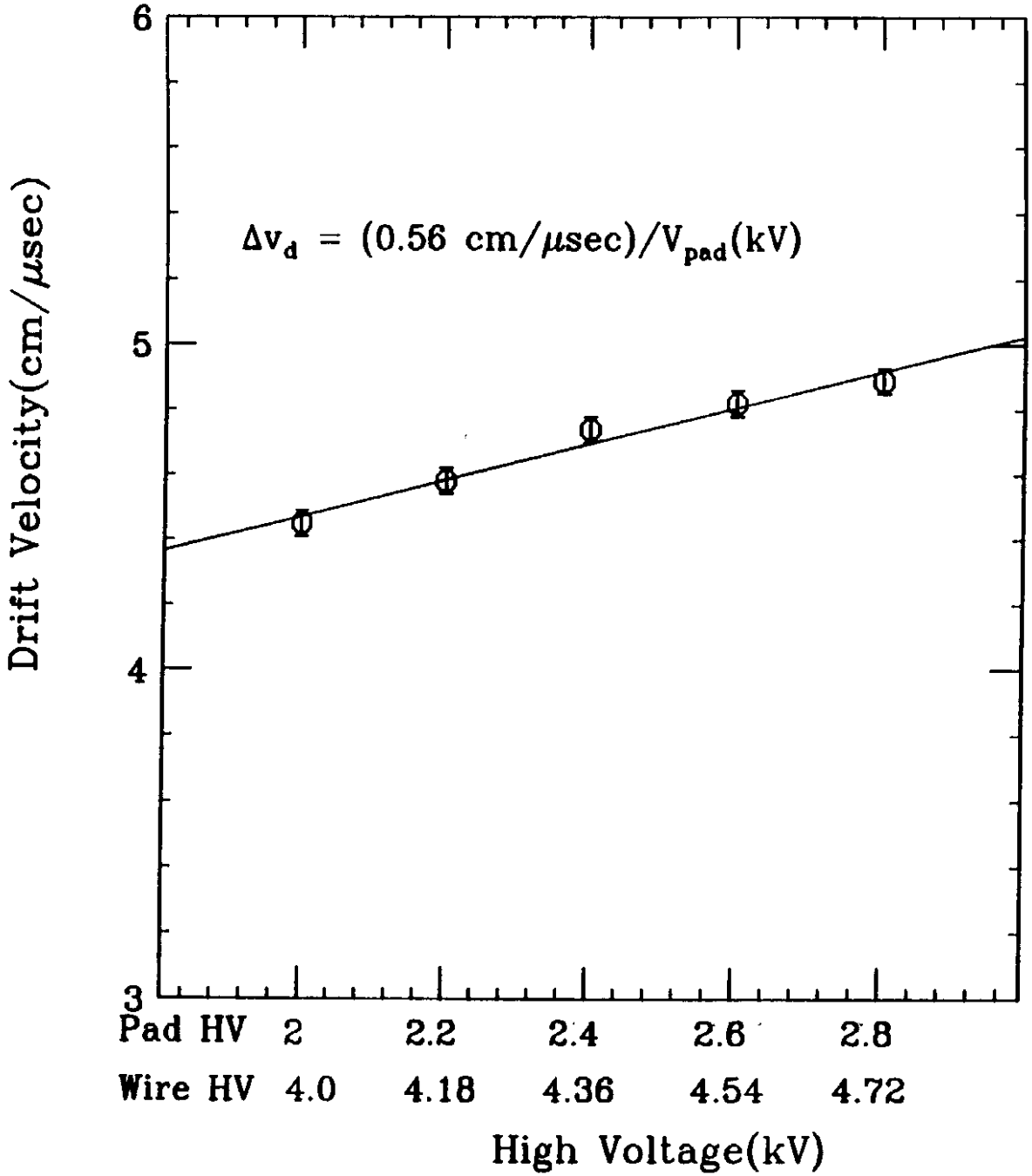
6
5
4
3
Drift Velocity(cm/μsec)
Δv_d = (0.56 cm/μsec)/V_pad(kV)
Pad HV 2 2.2 2.4 2.6 2.8
Wire HV 4.0 4.18 4.36 4.54 4.72
High Voltage(kV)

Fig. 5-a

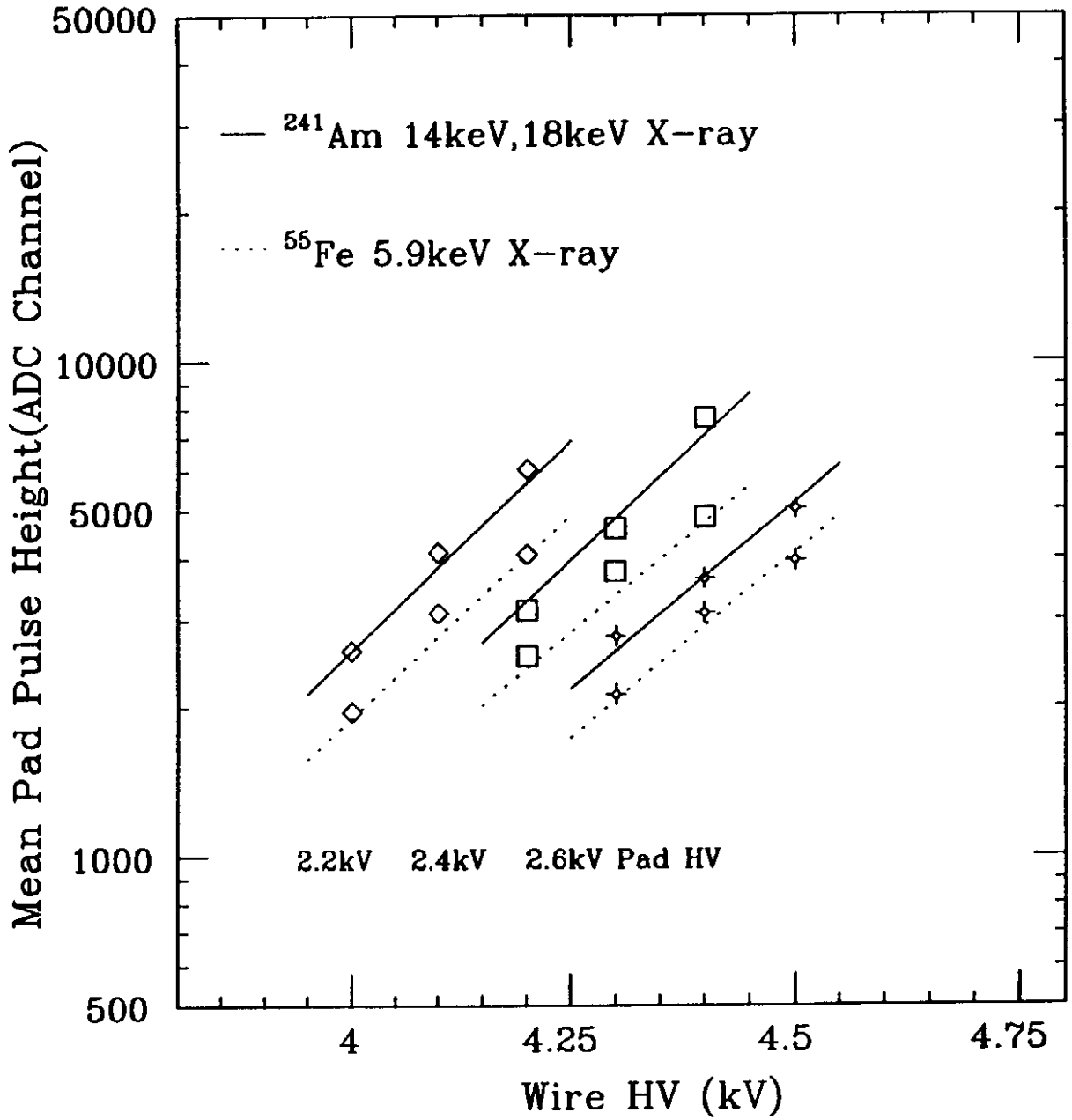
50000
10000
5000
1000
500
Mean Pad Pulse Height(ADC Channel)
^{241}Am 14keV,18keV X-ray
^{55}Fe 5.9keV X-ray
2.2kV 2.4kV 2.6kV Pad HV
4
4.25
4.5
4.75
Wire HV (kV)

Fig. 5-b

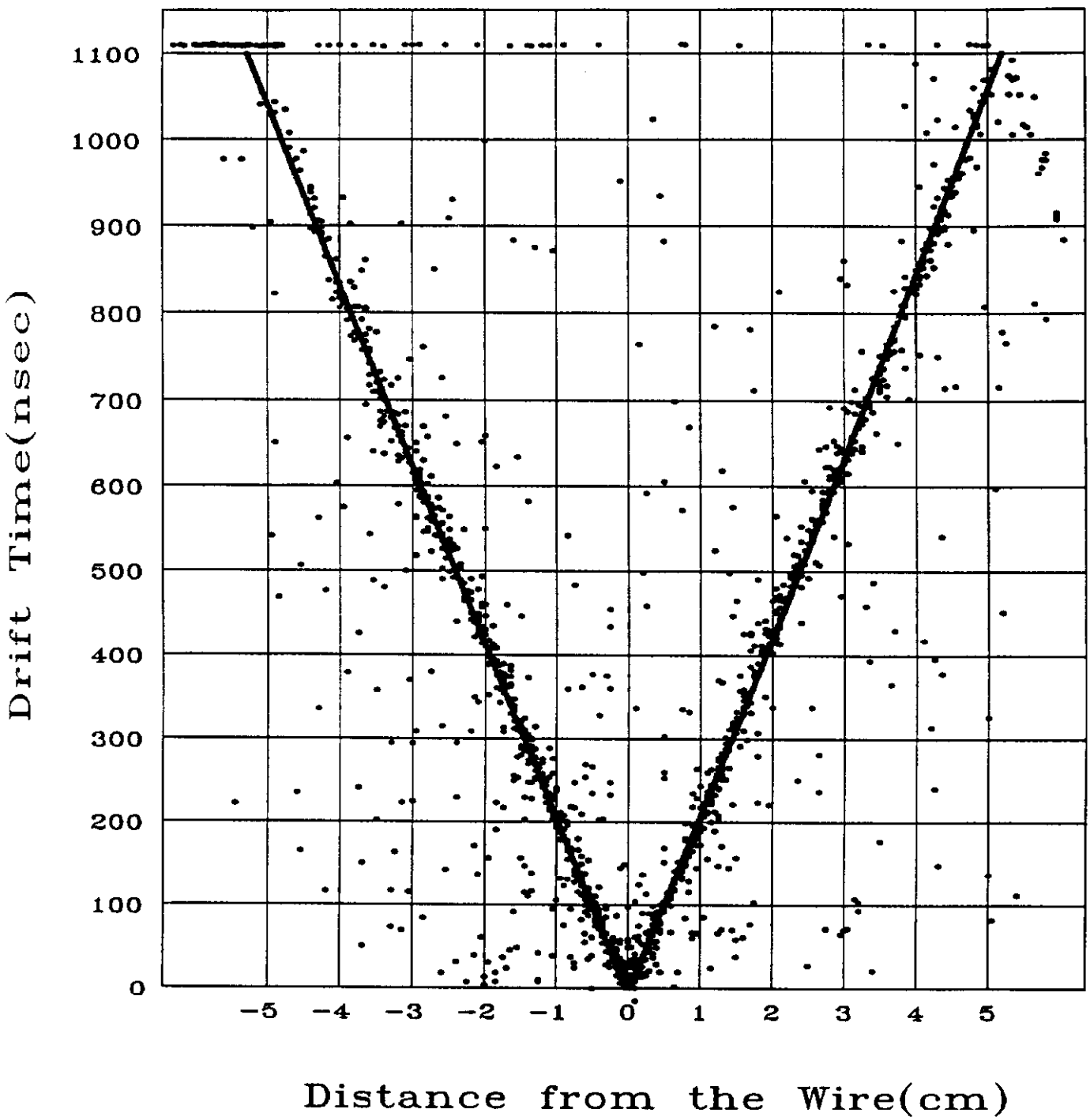
Drift Time(nsec)
1100
1000
900
800
700
600
500
400
300
200
100
0
−5
−4
−3
−2
−1
0
1
2
3
4
5
Distance from the Wire(cm)

Fig. 6

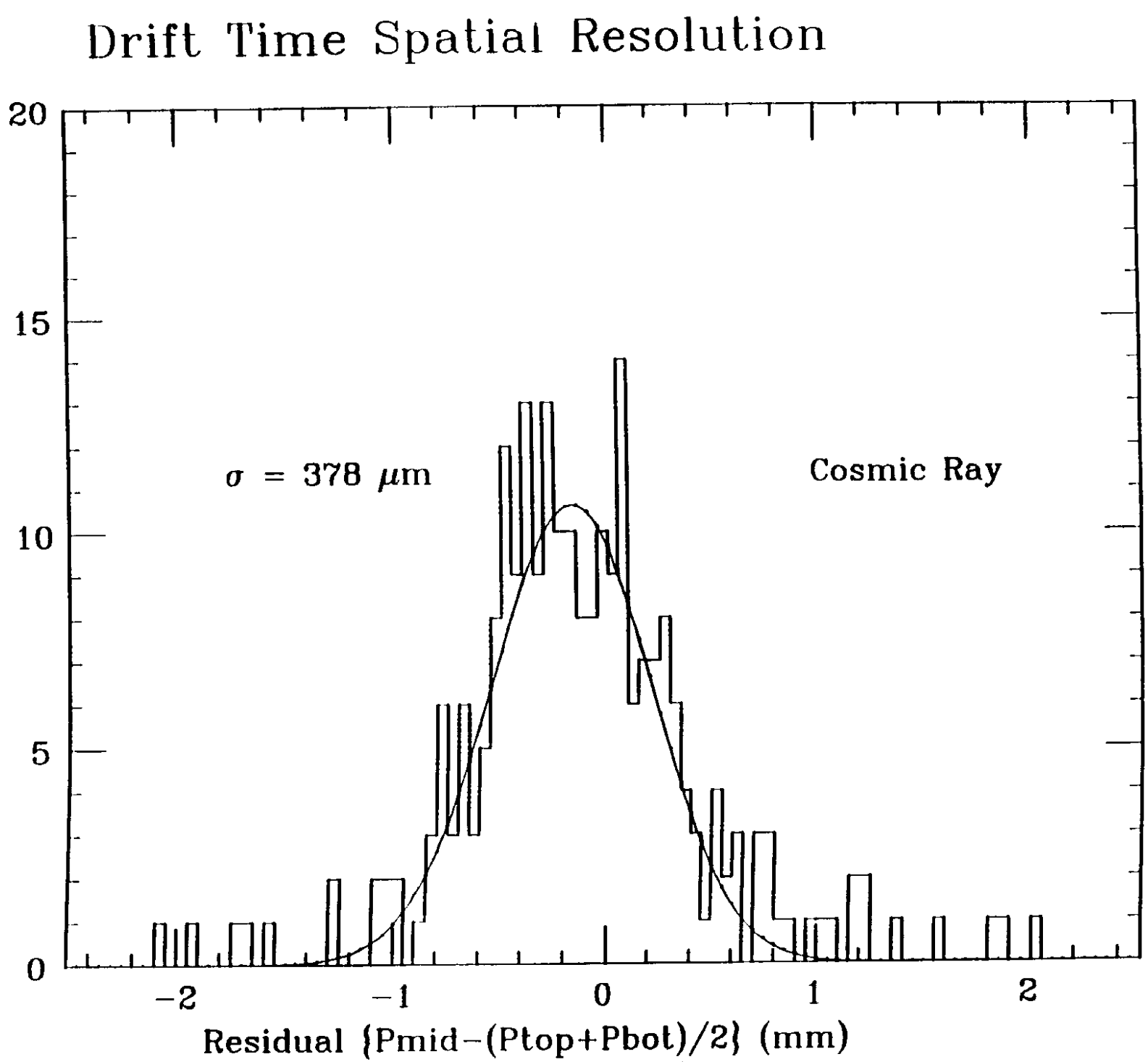
Drift Time Spatial Resolution
20
15
10
5
0
σ = 378 μm
Cosmic Ray
−2
−1
0
1
2
Residual {Pmid−(Ptop+Pbot)/2} (mm)

Fig. 7

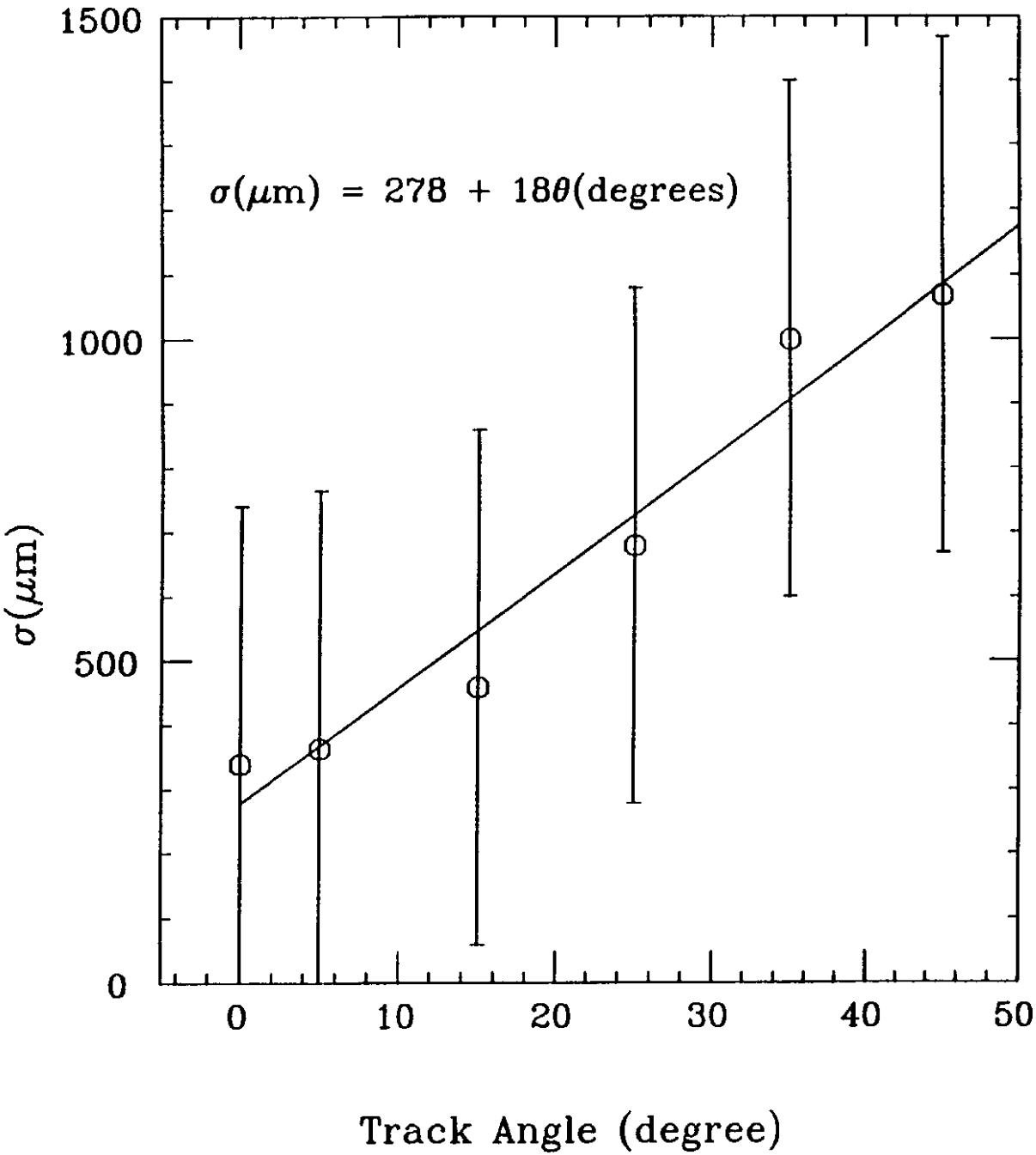
1500
1000
500
0
$\sigma(\mu m) = 278 + 18\theta(degrees)$
$\sigma(\mu m)$
0
10
20
30
40
50
Track Angle (degree)

Fig. 8

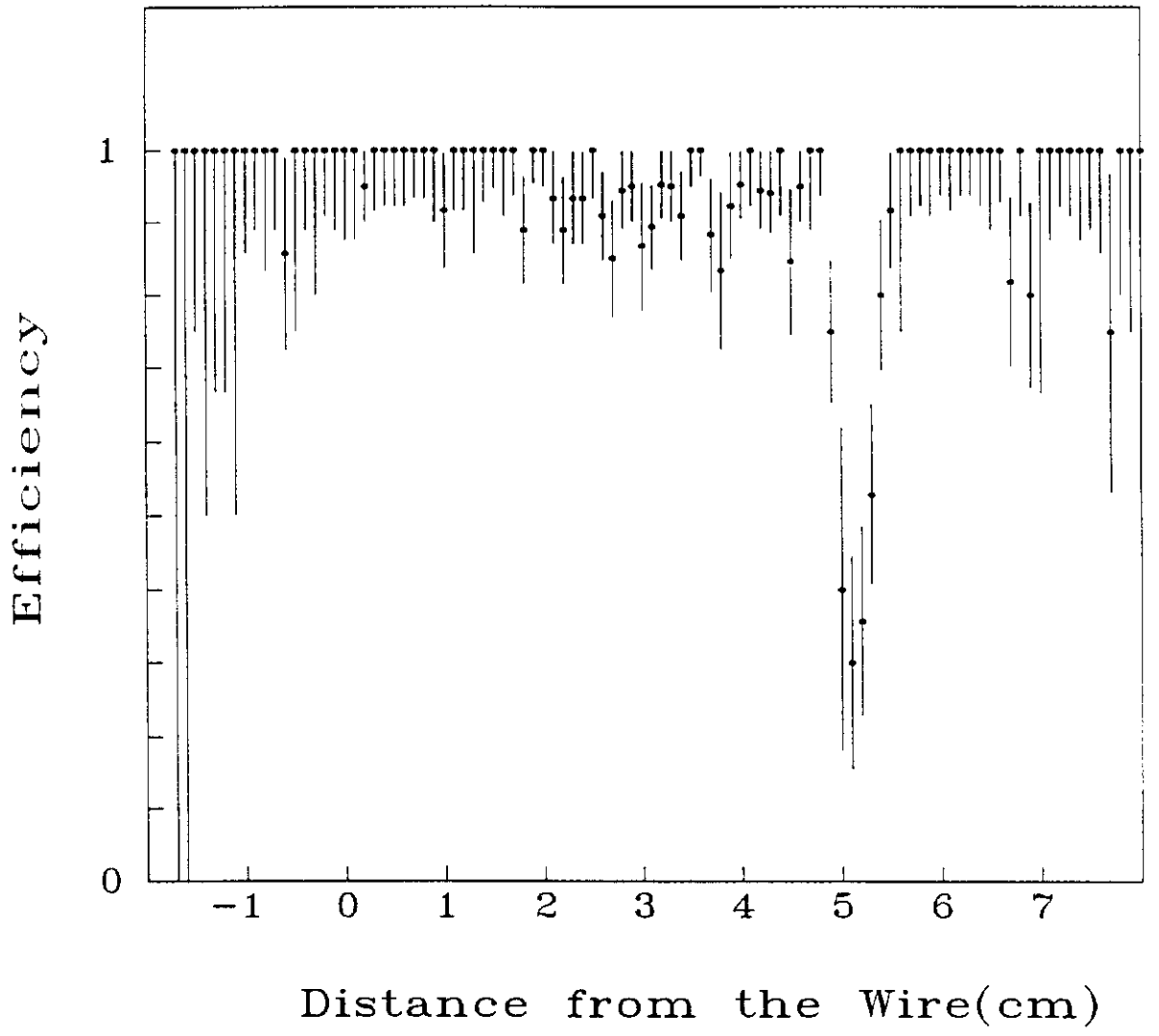

Fig. 9

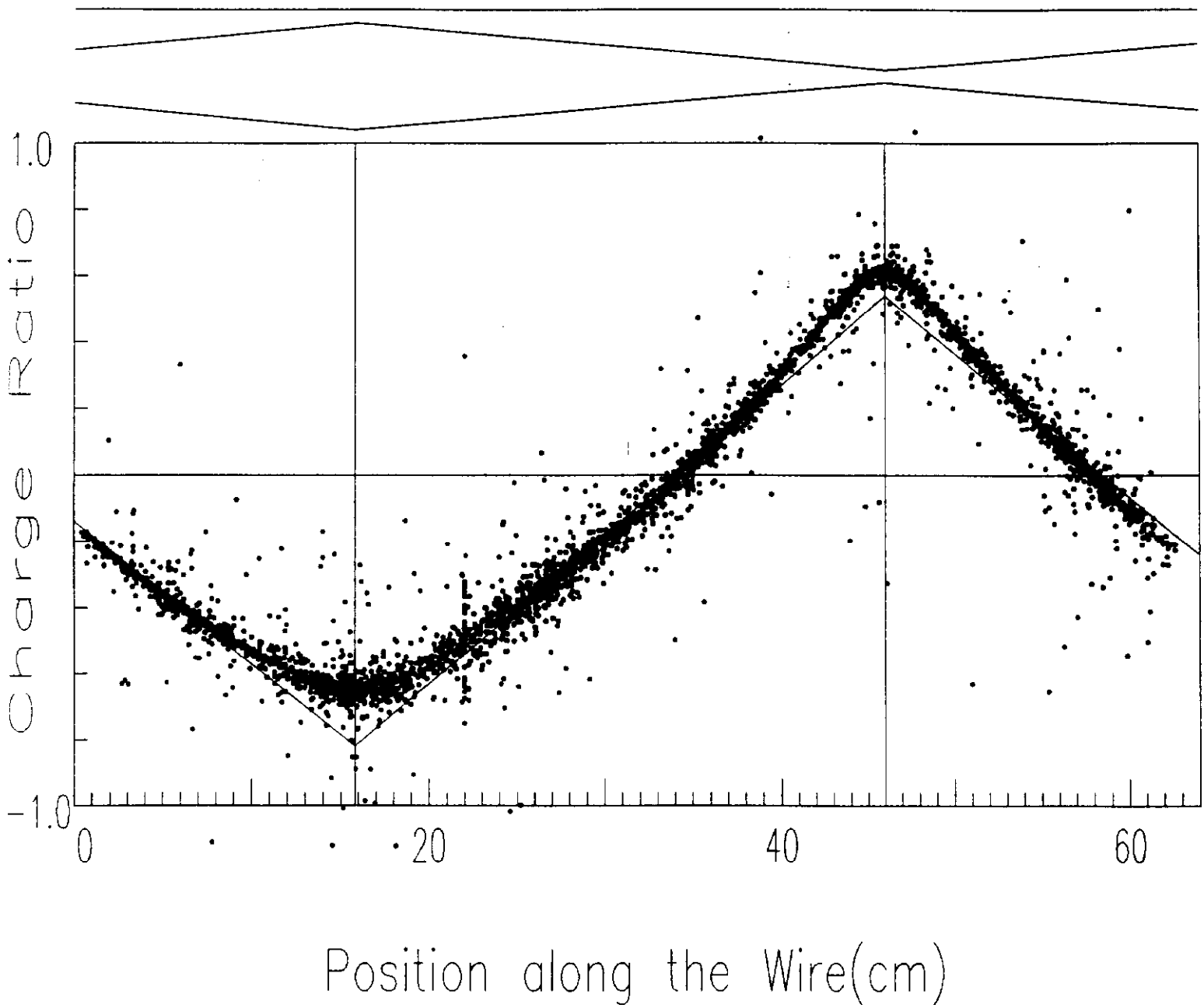

Fig. 10

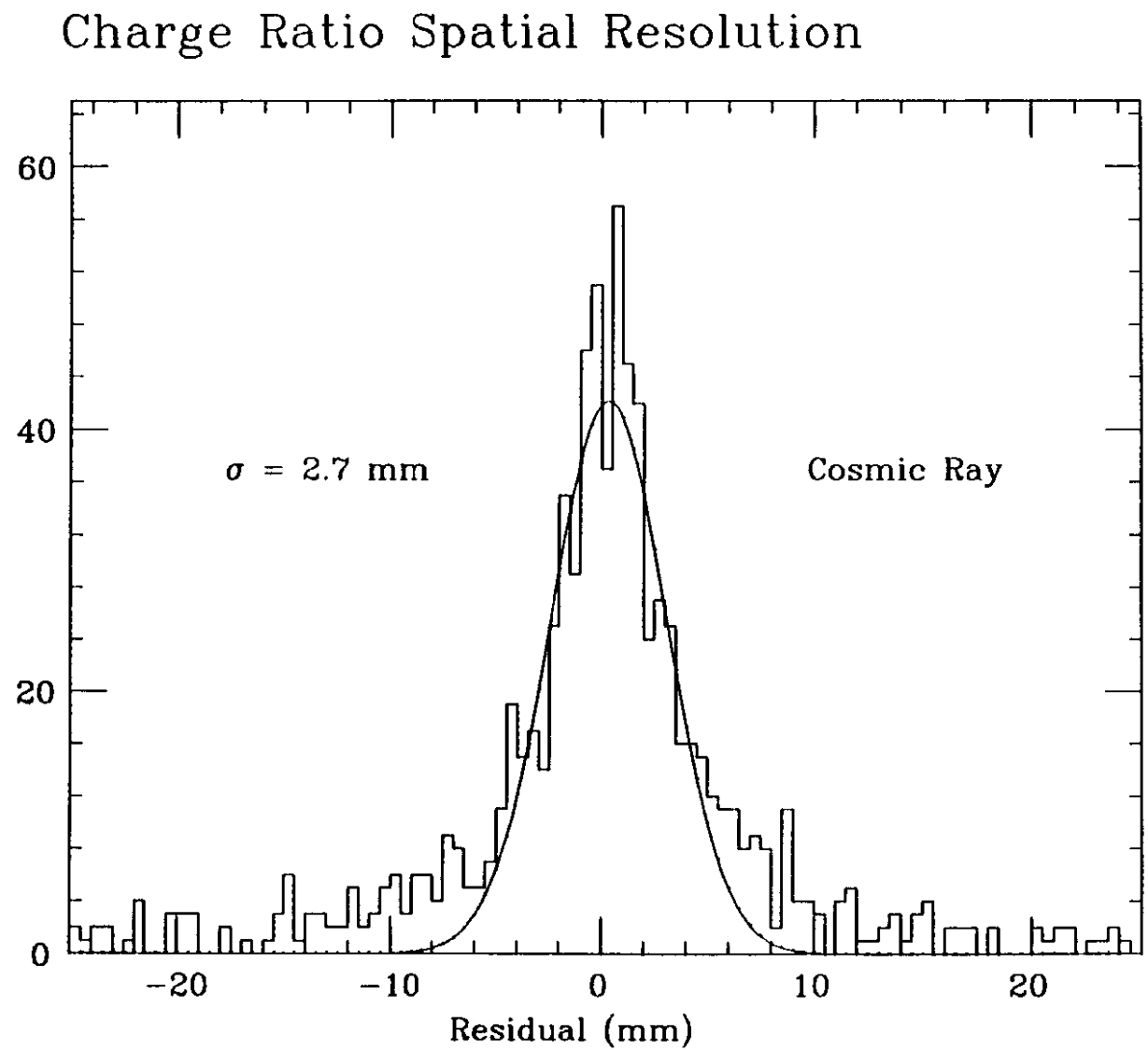
Charge Ratio Spatial Resolution
60
40
20
0
σ = 2.7 mm
Cosmic Ray
−20
−10
0
10
20
Residual (mm)

Fig. 11

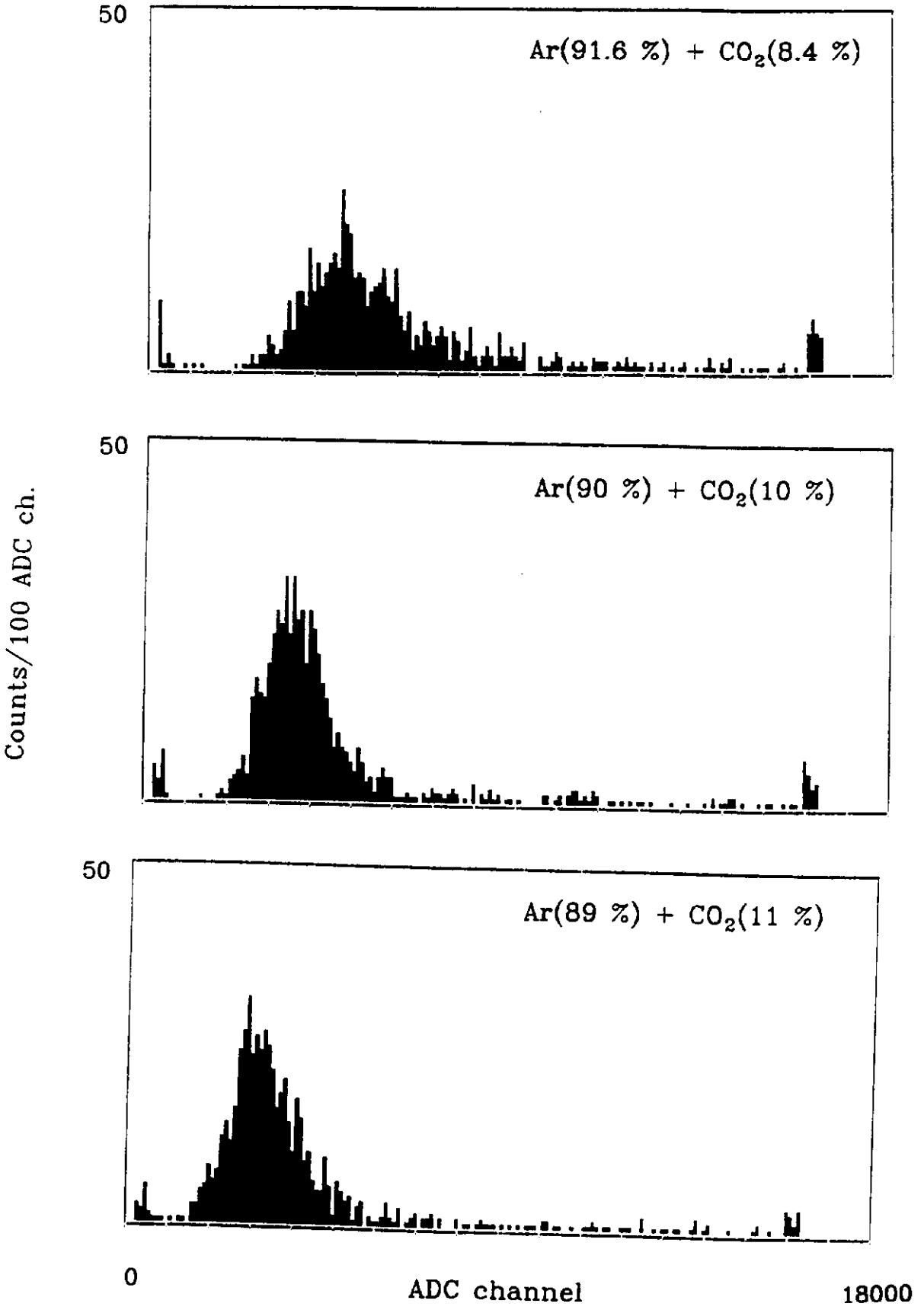
50
Ar(91.6 %) + CO_2(8.4 %)
50
Ar(90 %) + CO_2(10 %)
50
Ar(89 %) + CO_2(11 %)
Counts/100 ADC ch.
0
ADC channel
18000

Fig. 12

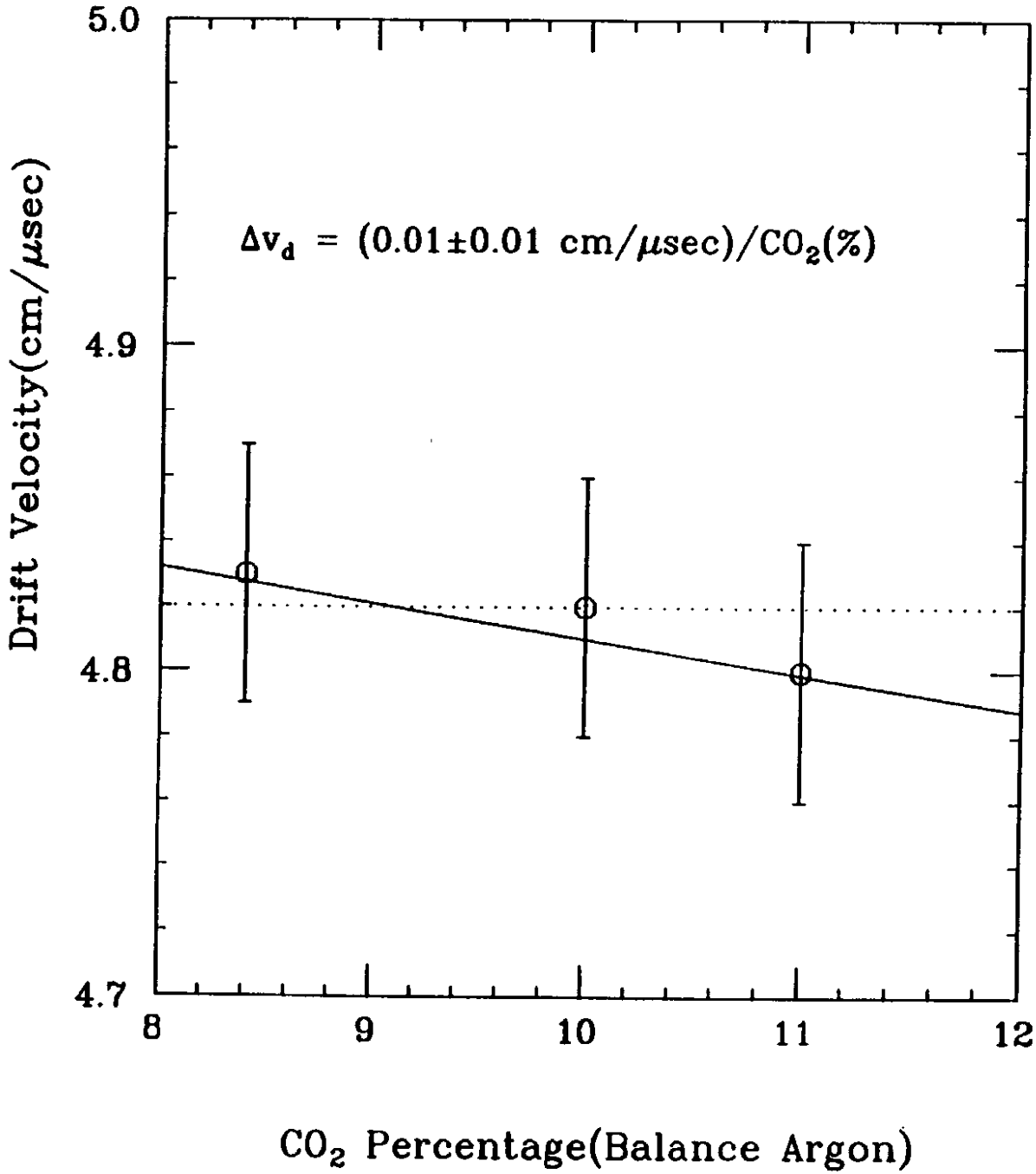
5.0
4.9
4.8
4.7
8
9
10
11
12
Drift Velocity(cm/μsec)
Δv_d = (0.01±0.01 cm/μsec)/CO_2(%)
CO_2 Percentage(Balance Argon)

Fig. 13

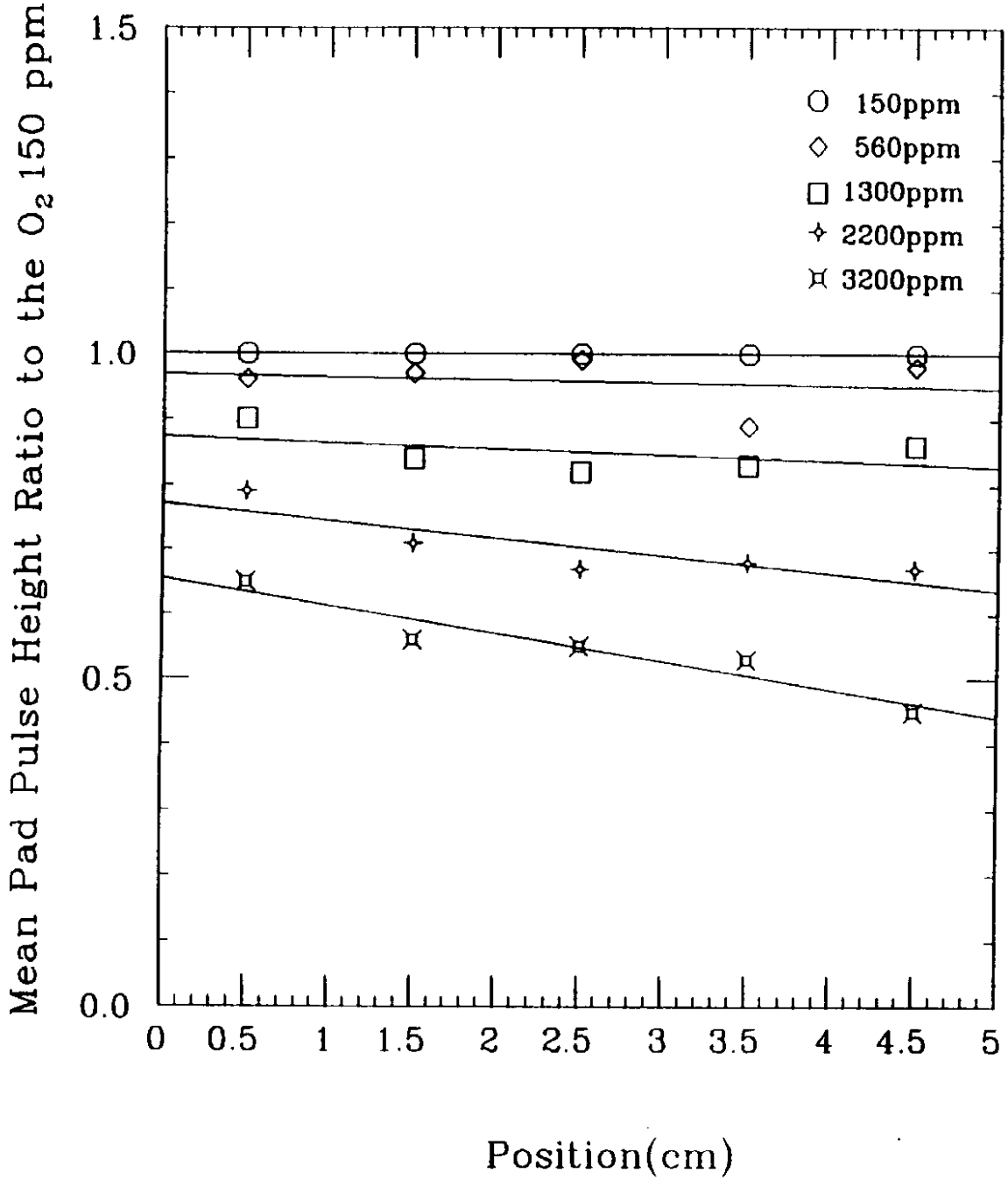
Mean Pad Pulse Height Ratio to the O_2 150 ppm
1.5
1.0
0.5
0.0
0
0.5
1
1.5
2
2.5
3
3.5
4
4.5
5
150ppm
560ppm
1300ppm
2200ppm
3200ppm
Position(cm)

Fig. 14

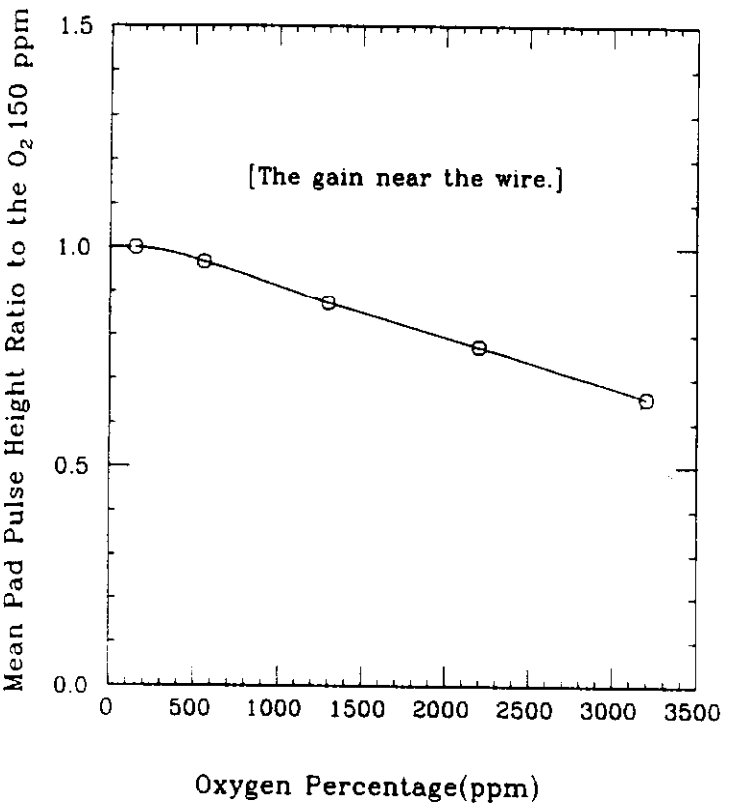
Mean Pad Pulse Height Ratio to the O_2 150 ppm
1.5
1.0
0.5
0.0
[The gain near the wire.]
0
500
1000
1500
2000
2500
3000
3500
Oxygen Percentage(ppm)

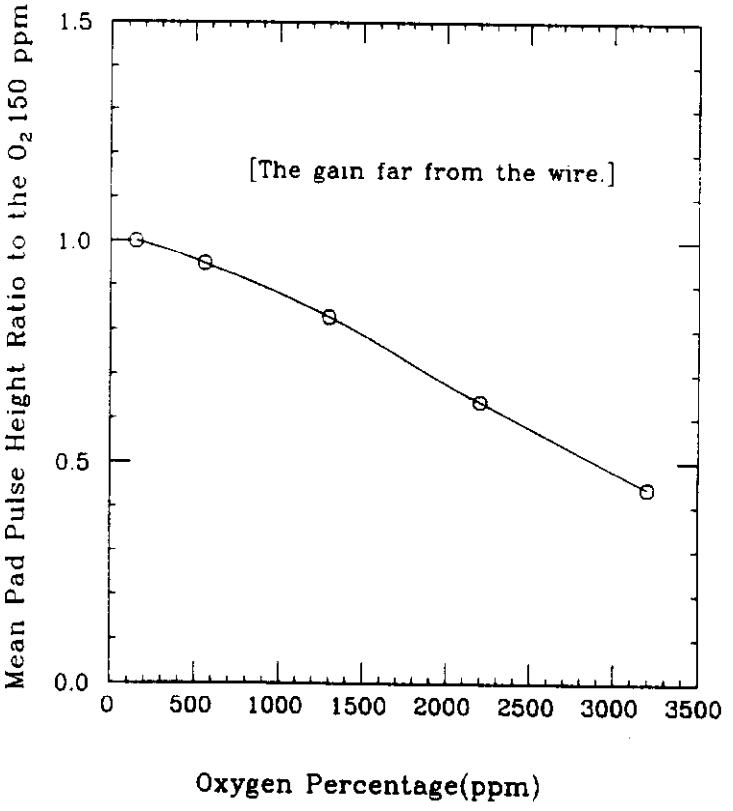
Mean Pad Pulse Height Ratio to the O_2 150 ppm
1.5
1.0
0.5
0.0
[The gain far from the wire.]
0
500
1000
1500
2000
2500
3000
3500
Oxygen Percentage(ppm)

Fig. 15